Position 170 of Rabbit Na^+/Glucose Cotransporter (rSGLT1) Lies in the Na^+ Pathway; Modulation of Polarity/Charge at this Site Regulates Charge Transfer and Carrier Turnover

Steven A. Huntley, Daniel Krofchick, and Mel Silverman
Department of Medicine, University of Toronto, Toronto, Ontario, Canada

ABSTRACT Positions 163, 166, and 173, within the putative external loop joining transmembrane segments IV and V of rabbit Na^+/glucose cotransporter, form part of its Na^+ interaction and voltage-sensing domain. Since a Q170C mutation within this region exhibits anomalous behavior, its function was further investigated. We used *Xenopus* oocytes coinjected with mouse T-antigen to enhance Q170C expression, and the two-microelectrode voltage-clamp technique. For Q170C, α-methyl D-glucopyranoside, phloridzin, and Na^+ affinity values are equivalent to those of wild-type; but turnover is reduced ~50%. Decreased [Na^+] reduces Q170C, but not wild-type, charge transfer. Q170C presteady-state currents exhibit three time constants, τ, identical to wild-type. MTSES decreases maximal α-methyl D-glucopyranoside-induced currents by ~64% and Na^+ leak by ~55%; phloridzin and Na^+ affinity are unchanged. MTSES also reduces charge transfer (dithiothreitol-reversible) and Q170C turnover by ~60–70%. MTSEA and MTSET protect against MTSES, but neither affect Q170C function. MTSES has no obvious effect on the τ-values. Q170A behaves the same as Q170C. The mutation Q170E affects voltage sensitivity and reduces turnover, but also appears to influence Na^+ interaction. We conclude that 1), glutamine 170 lies in the Na^+ pathway in rabbit Na^+/glucose cotransporter and 2), altered polarity and charge at position 170 affect a cotransporter conformational state and transition, which is rate-limiting, but probably not associated with empty carrier reorientation.

INTRODUCTION

The rabbit intestinal Na^+/glucose carrier (rSGLT1) is the first Na^+ cotransporter to have been cloned (Hediger et al., 1987), and serves as an excellent model system to explore the mechanisms of ion-coupled transport. The expression of cloned SGLT1 in *Xenopus* oocytes and the use of the two-microelectrode voltage-clamp technique have been particularly informative. Steady-state, sugar-induced inward Na^+ currents of the cotransporter yield affinity values for Na^+, and sugar substrate, as well as estimates of substrate coupling stoichiometry (Chen et al., 1996; Parent et al., 1992a). Presteady-state current traces, acquired in the presence of Na^+ (but not sugar substrate), are inhibited with either excess sugar, or the inhibitor phloridzin (pz). These current traces contain information about transition states involved in Na^+ binding/debinding, and reorientation of empty carrier across the membrane (Loo et al., 1993; Zampighi et al., 1995). The presteady-state currents are attributed to movement of Na^+ within the electric field of the membrane, and movement of charged residues of the empty cotransporter as it undergoes conformational transitions (Loo et al., 1993). The simplest model that has been proposed, as illustrated in Fig. 1 *A*, consists of two outward-facing conformational states: one with bound Na^+, *state 1*, and one without Na^+, *state 2*; and an inward-facing conformational state of empty carrier, *state 3*. According to this three-state model, there are two transitions, one involving Na^+ binding/debinding, and another involving reorientation of the empty cotransporter between outward- and inward-facing conformations. However, using the cut-open oocyte technique (Costa et al., 1994; Taglialatela et al., 1992), Chen et al. (1996) documented the existence of two distinct transitions of human SGLT1 (hSGLT1) in the complete absence of Na^+, implying that reorientation of empty carrier from outside to inside takes place in two steps rather than one. This evidence led to the revised four-state model, illustrated in Fig. 1 *B*.

Recently, Krofchick and Silverman (2003) performed a detailed analysis of rSGLT1 *OFF* currents. Using this experimental approach, complemented by computer simulation studies, the transient currents were characterized by a third-order exponential decay, yielding three time constants, thus supporting the four-state model. Although there now appears to be sufficient evidence that the number of

Submitted January 18, 2004, and accepted for publication April 5, 2004.

Address reprint requests to Mel Silverman, Medical Sciences Building, Room 7205, 1 King's College Circle, Toronto, ON, M5S 1A8, Canada. Tel.: 416-978-7189; Fax: 416-971-2132; E-mail: melvin.silverman@utoronto.ca.

Abbreviations used: αMG, α-methyl D-glucopyranoside; DTT, dithiothreitol; hSGLT1, human SGLT1; I_{max}, maximal substrate-induced current; k, turnover number; K_D, phloridzin affinity constant; K_M, substrate affinity constant; K_{Na}, Na^+ affinity constant; MTS, methanethiosulfonate; MTSEA, (2-aminoethyl)methanethiosulfonate hydrobromide; MTSES, Na^+(2-sulfonatoethyl)methanethiosulfonate; MTSET, [2-(trimethylammonium)ethyl]methanethiosulfonate bromide; n, Hill coefficient; pz, phloridzin; Q_{dep}, charge due to depolarizing pulses; Q_{hyp}, charge due to hyperpolarizing pulses; Q_{max}, the maximum charge transferred as calculated with the two-state Boltzmann relation; Q_{total}, the maximum charge transferred; rSGLT1, rabbit SGLT1; SGLT1, high affinity Na^+/glucose cotransporter; wt SGLT1, wild-type SGLT1; τ, decay constant; τ_s, slow decay constant; τ_m, medium decay constant; τ_f, fast decay constant; TM, transmembrane segment; $V_{0.5}$, potential at which charge transfer is half complete; V_h, holding potential; V_t, test potential; z, steady-state valence; z_{app}, apparent valence of charge movement.

0006-3495/04/07/295/16 $2.00

doi: 10.1529/biophysj.104.040253

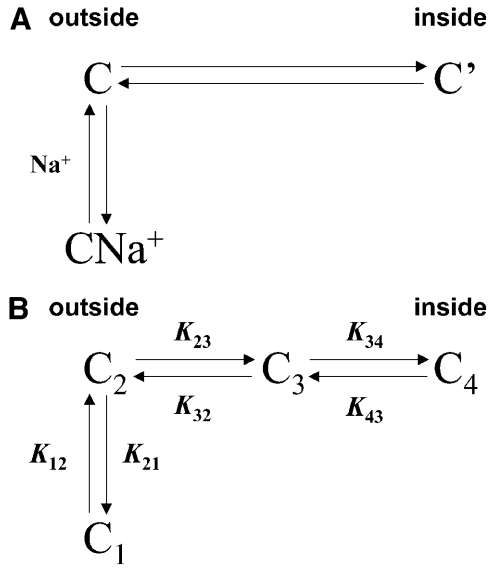

FIGURE 1 The state models of SGLT1 in the absence of sugar substrate. (*A*) Three-state system. The model is comprised of two outside-facing conformations, one with bound Na^+ (CNa^+ state) and one without (C state), and an inside-facing conformation (C' state). Three states necessarily have two transitions, a Na^+ binding/debinding transition involving either one ion or two simultaneous ions, $CNa^+ \Leftrightarrow C$, and an empty carrier transition, $C \Leftrightarrow C'$. (*B*) Four-state system. Model proposed by Chen et al. (1996) for hSGLT1, which introduced an intermediate empty carrier conformational state, C_3. Consequently, reorientation of empty carrier from inside facing to outside facing occurs with two transitions, $C_2 \Leftrightarrow C_3$, $C_3 \Leftrightarrow C_4$. The rate constants for the transitions are displayed.

transitions associated with the presteady-state currents of SGLT1 is greater than originally assumed (Loo et al., 1993), the region(s) of the cotransporter that are implicated in these transitions remains unknown.

Site-directed mutagenesis, as well as comparison of the functional behavior of wt SGLT1 from different species, have helped identify amino acids of functional importance in the Na^+/sugar cotransport (Panayotova-Heiermann et al., 1994). Moreover, the C-terminal half of the transporter, specifically the region involving transmembrane segments (TMs) X–XIII, has been implicated in sugar permeation (Panayotova-Heiermann et al., 1997, 1996). Several years ago, our laboratory began to use cysteine-scanning mutagenesis and the substituted cysteine accessibility method as a strategy to identify functional domains of rSGLT1. The studies determined that a region localized to the putative loop joining TMs IV and V is involved in the Na^+ binding and voltage-sensing properties of rSGLT1, particularly residues 163, 166, and 173 (Lo and Silverman, 1998a,b; Vayro et al., 1998). Further, the 166 residue was demonstrated to influence empty carrier kinetics (Lo and Silverman, 1998b). However, in this same region, one loop mutant, Q170C, displayed unique functional behavioral characteristics compared to F163C, A166C, and L173C. For example, whereas F163C, A166C, and L173C were each inhibited by reaction with the cationic MTS derivative 2-aminoethyl methanethiosulfonate (MTSEA) but not MTSES (Lo and Silverman, 1998a), Q170C was inhibited by reaction with MTSES, but not MTSEA. Moreover, MTSES reaction with Q170C appeared to affect charge transfer rather than Na^+ binding.

Complete characterization of Q170C was limited in our earlier studies by the fact that measured charge transfer in the presence of MTSES was too low to permit quantitative evaluation of this phenomenon. To overcome this difficulty, we coinjected mouse T-antigen along with Q170C cDNA, and obtained 2.5-fold-enhanced expression of Q170C compared to the cDNA injection protocol used previously. The improved Q170C levels of expression were comparable to those of wt rSGLT1, therefore altered transporter function due to overexpression is unlikely. Using this approach we undertook a thorough examination of all steady-state and presteady-state parameters to extend our earlier work on Q170C, and achieve a comprehensive functional characterization. In the present study we confirm our earlier finding (Lo and Silverman, 1998a), that the glutamine-to-cysteine mutation at position 170 exerts little influence over the cotransporter's affinity for Na^+, αMG, or phloridzin. However, our new data show that the mutation reduces cotransporter turnover by 50% and elicits profound changes in its presteady-state behavior. Furthermore, lowering external [Na^+] progressively decreases charge transfer of Q170C at depolarizing potentials, without proportionately increasing charge transfer at hyperpolarizing potentials. By comparison, for wt rSGLT1, reducing external [Na^+] shifts the $V_{0.5}$ of the Boltzmann without affecting total charge transferred. This suggests that the mutation has altered some rate-limiting transition step(s). When analyzed using the new *OFF* current protocol (Krofchick and Silverman, 2003), Q170C presteady-state currents demonstrate a third-order, rather than a single-order, exponential decay—characterized by three time constants, τ_s (slow), τ_m (medium), and τ_f (fast), with similar values to that documented for wt rSGLT1 (Krofchick and Silverman, 2003).

Taking advantage of the increased levels of Q170C expression resulting from coinjection of mouse T-antigen cDNA, an extensive assessment of the effects of MTSES on steady-state and presteady-state behavior of Q170C was performed. Introduction of the negatively charged ethylsulfonate at residue 170, after reaction with anionic MTSES, causes marked reduction in steady-state sugar-induced inward Na^+ currents, without affecting Na^+ or sugar substrate affinity. In contrast, chemical modification of Q170C with either cationic MTSEA or membrane impermeant MTSET does not alter transporter function. However, exposure to MTSEA or MTSET blocks the effects of anionic MTSES. MTSES also significantly reduces the Q170C Na^+ leak. After reaction with MTSES there is a marked reduction of charge transfer at depolarizing potentials that is not recovered at hyperpolarizing voltages—similar to observations for Q170C when the Na^+ concentration is reduced by a factor of 10. Previously, it was reported that MTSES has

little effect on Q170C turnover (Lo and Silverman, 1998a); however, these earlier studies were made difficult by the fact that in the presence of MTSES, the Q170C currents are reduced to low levels, thereby compromising measurement accuracy. By taking advantage of enhanced expression achieved through coinjection of T-antigen, we now show that reaction with MTSES causes a 60–70% reduction in Q170C turnover. Thus, Q170C reacted with MTSES has a turnover number which is less than one-fourth of wt rSGLT1 turnover. Interestingly, although charge transfer is significantly retarded after MTSES exposure, the observed values for the three τ-measurements, which characterize Q170C presteady-state behavior, are not obviously changed.

Q170A and Q170E rSGLT1 mutants were employed to add further evidence that polarity and charge at the 170 residue affect transporter turnover. Presteady-state experiments revealed that Q170A behaves almost identically with Q170C, and also exhibits reduced turnover. Q170E, on the other hand, appears to have a similar but less pronounced effect compared to Q170C post-MTSES—voltage sensitivity was affected, and turnover reduced, but not to the same extent as with MTSES. Q170E also provided the first evidence of Na^+ interaction at position 170.

It therefore appears that modulation of polarity and charge at the 170 glutamine position, specifically introduction of a negative but not positive charge, critically reduces carrier turnover and charge transfer, and can influence Na^+ interaction. Interestingly, both the Q170C mutation, and subsequent reaction with MTSES significantly reduce turnover, yet neither alters the investigated time constants—suggesting that a transporter conformational transition is affected, which is rate-limiting but probably not associated with transmembrane reorientation of empty carrier.

MATERIALS AND METHODS

Molecular biology

The eukaryotic expression vector pMT3 (provided by the Genetics Institute, Boston, MA) was treated with *Pst*I and *Kpn*I to extract the multiple cloning site, generating pMT4. The cDNA of rSGLT1 (provided by M. Hediger) was subcloned into the remaining *Eco*RI site. The Q170C, Q170A, and Q170E mutations were generated via the megaprimer protocol of polymerase chain reaction mutagenesis as described previously and confirmed by sequencing (Lo and Silverman, 1998a).

Oocyte preparation

Xenopus laevis were anesthetized in 0.2% aqueous solution of 3-aminobenzoic acid ethyl ester. Gravid ovarian sacs were removed, then carefully drawn to expose oocytes and allow access to solution. The oocytes were digested for 25–60 min with 2 mg/ml of type IV collagenase (Sigma, Oakville, ON, Canada). Collagenase was dissolved in Modified Barth's Saline (MBS) solution supplemented with MgCl. MBS/Mg^{2+} consists of 0.88 mM NaCl, 1.0 mM KCl, 2.4 mM $NaHCO_3$, 15.0 mM HEPES-NaOH, 1.0 mM $MgCl_2$, pH 7.4. Post-harvest/digestion care involved Leibovitz solution (Sigma) supplemented with 10 mM HEPES, 20 mg gentamycin, and 0.184 g L-glutamine, pH 7.4 with 10 mM NaOH.

Oocyte injection

Q170C rSGLT1 cDNA was delivered to the nucleus, via the animal pole, of the defolliculated oocytes at a concentration of 60 ng/μl. The injected oocytes were stored at 16–18°C for four or more days in Leibovitz solution of the same composition as that used immediately after collagenase treatment. To enhance expression of the rSGLT1, the rSGLT1 pMT4 plasmid was coinjected with a plasmid bearing the mouse plasmid LFI gene for large T-antigen, middle T-antigen, and small T-antigen at a concentration of 20 ng/μl.

Two-microelectrode voltage-clamp

Voltage-clamping and recordings were performed using a GeneClamp 500 amplifier, Digidata 1200B interface, and pClamp 6.0 data acquisition software (Axon Instruments, Union City, CA). Oocytes were impaled with 150-μm borosilicate glass capillary tubes (World Precision Instruments, Sarasota, FL). The capillary tubes were filled with 3 M KCl solution. Oocytes with resting potentials more positive than −30 mV were discarded. Eligible oocytes were constantly superfused with a voltage-clamping solution consisting of 100 mM NaCl, 2 mM KCl, 1 mM $MgCl_2$, 1 mM $CaCl_2$, and 10 mM HEPES-Tris base (pH 7.4). This voltage-clamping solution was used for all experiments, with the exception of Na^+ titrations and certain presteady-state experiments, which examined Na^+ dependence. The rate of superfusion was ~3.5 ml/min. The oocyte was held at a holding potential, V_h, of −50 mV, then was subjected to a series of voltage test pulses, V_t. The current responses were recorded with a sampling interval of 200 μs for steady-state experiments, 25 μs for the ramp protocol, and 20 μs for decay analysis. The traces represent presteady-state currents generated by the cotransporter, in response to stepping the voltage from the holding potential of −50 mV through a range of test pulses from −150 mV to +90 mV, in 10- or 20-mV increments. The *OFF* currents represent the reciprocal current responses when the voltage step is discontinued and returned to the holding potential, −50 mV. For those experiments, which required a more accurate measurement of charge transfer, the step function test pulse was replaced by a 5-ms ramp (Krofchick and Silverman, 2003). The array of ramp pulses mirrors that of the step protocol. The ramp protocol avoids conditions of measuring apparatus saturation, which typically occurs at early times of the step clamp, when large capacitive currents are produced. Thus, the ramp protocol ensures complete recovery of charge transfer over the entire range of voltages, including the extreme range of depolarizing and hyperpolarizing potentials.

Steady-state parameters were determined with the difference in the steady-state currents obtained before and after exposure to the substrate of interest. Steady-state currents were acquired with test pulses of 300-ms duration. The final 150 ms of a test pulse were selected and the average current value of this range was acquired. The average current values were plotted versus [substrate] and the following equation was fit to the curve,

$$I = I_{max} \times [S]^n / ([S]^n + K_{0.5}^n), \quad (1)$$

where S is the substrate of investigation (Na^+, αMG), I_{max} is the maximal current induced at saturating [substrate], n is the Hill coefficient, and $K_{0.5}$ is the Michaelis constant, which is the *[S]* at which the $I = I_{max}/2$, which serves as an approximation of substrate affinity. The calculation of substrate affinity values used the I_{max} values of −150 mV test pulses.

The presteady-state current of an expressing oocyte is comprised of both a nonspecific component, due to oocyte membrane capacitance, and an SGLT1-specific component. Isolation of the SGLT1-specific component was accomplished with phloridzin (pz), which is an SGLT1 inhibitor. The current recordings acquired in the presence of saturating pz (200 μM) were subtracted from the recordings acquired in the absence of pz, to provide the current due exclusively to rSGLT1. Presteady-state experiments used test pulses of the same values as those used for steady-state experiments; however, the test pulses were of a 150-ms duration. Baseline correction for

each trace was accomplished by subtracting the average values for the currents measured in the steady-state region (beyond 100 ms). The rSGLT1 presteady-state currents for each V_t were integrated over the entire course of the trace to calculate the total charge transferred by the cotransporter. The charge, Q, was plotted as a function of the test pulses, and these $Q(V_t)$ curves were fitted to the two-state Boltzmann relation,

$$Q = -N \times e \times z/(1 + \exp(z \times u \times (V_t - V_{0.5})) + Q_{dep}), \quad (2)$$

where Q is the total charge transferred, Q_{dep} is the charge due to depolarizing pulses, e is the elementary charge, z is the apparent valence of the movable charge, $V_{0.5}$ is the potential at which half of the total charge transfer is complete, and N is the number of cotransporters expressed at the surface. The term $u = F/RT$; F is Faraday's constant, R is the gas constant, and T is absolute temperature.

The initial mathematical operations were performed with Clampfit (Axon Instruments). Results were filtered via a 1-kHz, 5-point Gaussian filter. Additional curve fitting was performed in ORIGIN 6.0 with the Levenberg-Marquardt algorithm.

Transient current measurement

Transient decay parameters of Q170C *OFF* currents were derived with the protocol illustrated in Fig. 2, and described in detail by Krofchick and Silverman (2003). The holding potential, V_h, was −50 mV; this potential was maintained between experiments. From −50 mV, the potential was stepped to an array of pre-step potentials, or *ON* potentials. The pre-step potentials were from −150 mV to 90 mV in 10-mV increments, and were applied for a 100-ms duration, to allow the system to equilibrate. At $t = 0$ ms, the desired post-step potential, or *OFF* potential, was applied. A set of post-step potentials was used, from −150 mV to 90 mV in 20-mV increments; the representative waveform of Fig. 2 *A* has a post-step potential of 50 mV. The post-step potential is applied for a 100-ms duration, from $t = 0$ ms to $t = 100$ ms. The resulting array of post-step transient currents, generated with the waveform described, is analyzed for presteady-state parameters. The settling time of the voltage-clamp was determined by measuring the oocyte membrane potential as a function of time. Voltage steps, ranging from 70 mV to 240 mV, were investigated. Final potentials were attained 0.6 (70 mV jump) to 1.3 ms (240 mV jump) after the onset of the clamp. Transient currents before the settling of the clamp were removed before fitting.

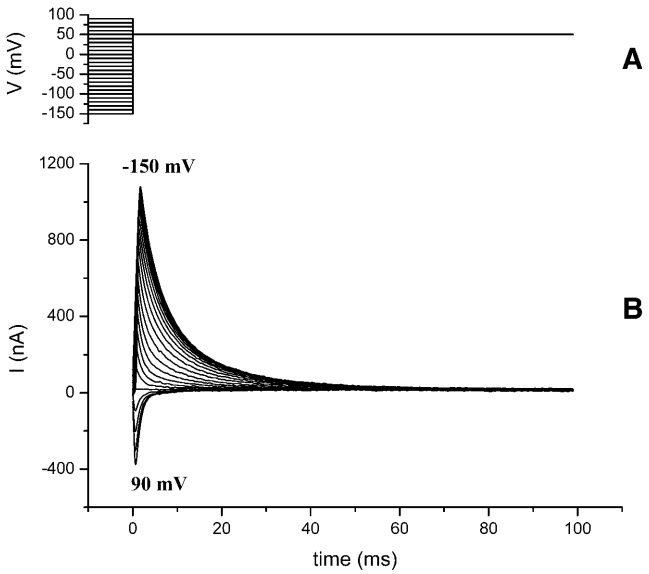

FIGURE 2 Representative transient *OFF* currents of Q170C rSGLT1 for a 50-mV post-step potential. (*A*) The waveform used to generate the Q170C transient currents, displayed in *B*. The pre-step potentials were from −150 mV to 90 mV, in 10-mV increments, and were applied for a 100-ms duration before the step at $t = 0$, to allow the system to stabilize. At $t = 0$ ms, the desired post-step potential was applied; the representative waveform of *A* has a post-step potential of 50 mV. The post-step potential is applied for a 100 ms duration, from $t = 0$ ms to $t = 100$ ms. (*B*) An array of Q170C rSGLT1 post-step transient currents, generated with the waveform described in *A*.

Fitting decay currents

Each current trace of a post-step potential was fitted, from 0 to 100 ms, to a first-order exponential decay, a second-order exponential decay, and a third-order exponential decay. The order of exponential decay at which the χ^2 value demonstrated no change, or at which the higher order terms became meaningless, was discarded for the previous order of decay. Extremely large or small time constants, amplitude values or large error values associated with such parameters, precluded the validity of a particular order of decay. Several criteria were considered when deciding upon an order of decay. Typically, higher order of decay was accepted if its χ^2 value decreased by ~10% or more compared to the previous lower order fit. Also, a higher order fit was only deemed valid if the trends observed for such parameters as time constants and amplitude values were consistent over a range of post-step potentials (Krofchick and Silverman, 2003). Finally the residuals had to demonstrate a definitive improvement at the highest order fit. The complete details of the technique are provided by Krofchick and Silverman (2003).

Statistical comparisons of means

The mean values of parameters are presented with standard deviation (mean ± SD). Comparisons of parameters, drawn between wild-type and Q170C rSGLT1, were tested with a two-sample *t*-test for independent samples with equal variances. Comparisons of parameters, before and after exposure to sulfhydryl specific compounds in the same oocyte, were tested with the paired *t*-test.

Tissue culture

COS-7 cells were grown and maintained in RPMI 1640 medium (Invitrogen Canada, Burlington, ON). The RPMI 1640 was supplemented with 21 mM $NaHCO_3$, 25 mM HEPES/NaOH, pH 7.4, 10% fetal calf serum, and 50 units/ml antibiotic solution containing penicillin/streptomycin. Cells were maintained in a 5% CO_2 atmosphere at 37°C.

Cell transfection

At 70% confluency, the COS-7 cells were transfected with Lipofectamine Plus (Invitrogen) according to manufacturer's protocol.

αMG uptake experiments

Uptake was gauged with [^{14}C]α-MG (Amersham Health, Oakville, ON, Canada) with a specific radioactivity of 293 mCi/mmol. Culture medium was aspirated, and replaced with 500 μL of incubation medium containing either 140 mM NaCl or 140 mM KCl, 20 mM mannitol, 10 mM HEPES/Tris, pH 7.4 and 1 mM [^{14}C]α-MG. After 10 min at room temperature, the incubation medium was aspirated and the wells were washed three times with 3 mL of ice-cold stop buffer, consisting of 140 mM KCl, 20 mM mannitol, 10 mM HEPES/Tris, pH 7.4, and 200 μM phloridzin. The cells

were solubilized with 500 mL of PBS buffer with 0.1% SDS. Solubilization proceeded for 20 min, then the solution was removed and prepared for liquid-scintillation counting.

Phloridzin binding experiments

Phloridzin binding was gauged with [^{3}H]phloridzin (Sigma) with a specific radioactivity of 55 Ci/mmol. The transfected plates were removed from the incubator. The medium in the wells was aspirated, and replaced with 500 μL of incubation medium at room temperature. The incubation medium consisted of 140 mM NaCl, 20 mM mannitol, 10 mM HEPES/Tris at pH 7.4, and various concentrations of phloridzin. The phloridzin concentrations examined were 0.01, 0.05, 0.1, 0.3, 0.4, 0.5, or 1.0 μM. The incubation period was 1 min. The solubilization procedure was identical to that described for uptake experiments.

RESULTS

The effects of the glutamine-to-cysteine mutation at 170

Steady-state behavior of Q170C

As described in Materials and Methods, 300-ms test pulses are routinely employed in steady-state experiments, and the steady-state currents are analyzed over the time frame from 150 ms to 300 ms. These protracted currents allow optimized determination of the average current value during the steady-state region of the traces. The αMG-induced inward Na^+ currents of Q170C were measured over a range of αMG concentrations; each αMG bathing solution had a saturating [Na^+] of 100 mM. The resulting current (I) versus voltage (V_t) curves were transformed to I versus [αMG], and the Michaelis-Menten relationship was then fitted to these curves. The average αMG K_M for Q170C, from $V_t = -150$ mV to -90 mV, is 0.10 $\pm$ 0.01 mM ($n = 4$), which confirms our earlier findings (Lo and Silverman, 1998a), and is comparable to the value of 0.15 $\pm$ 0.024 mM obtained for wt SGLT1 over the same potential range (Lo and Silverman, 1998a). At the more negative test pulses, from -150 mV to -90 mV, there is little or no voltage dependency. However, voltage dependence is evident from -70 mV to -10 mV, similar to the αMG K_M voltage dependency of wt SGLT1 (Lo and Silverman, 1998a,b).

We next expanded our investigation of Q170C to examine the interaction with Na^+. The current versus [Na^+] curves (obtained at saturating 10 mM αMG), for a representative expressing oocyte, are displayed in Fig. 3 *A*. The Hill equation was fitted to these curves, for five oocytes, which permitted the derivation of the Hill coefficients and the Na^+ affinity values (K_{Na}). The Hill coefficients display a voltage dependence with values of 1.5 $\pm$ 0.20 to 2.3 $\pm$ 0.24, over the voltage range -150 mV to -10 mV ($n = 5$), suggesting that Q170C has a stoichiometry of at least two Na^+/transport cycle, the same as wt SGLT1. The Q170C K_{Na} values and voltage dependencies are similar to those of wt rSGLT1, as observed in our lab (data not shown) and as published

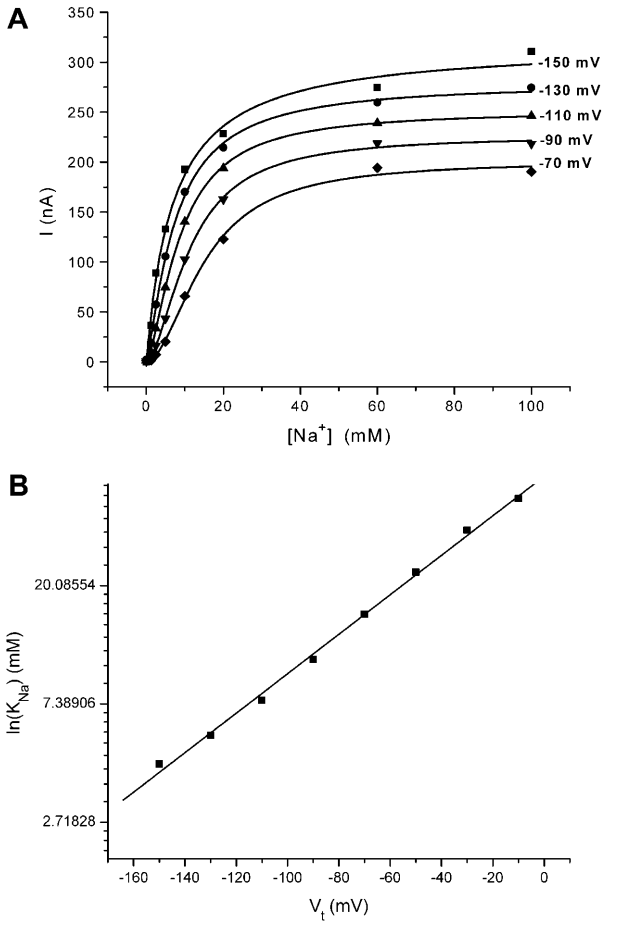

FIGURE 3 Steady-state kinetics of Q170C: determination of K_{Na}. Expressing oocytes were voltage-clamped and Na^+ titrations were performed using solutions with Na^+ concentrations ranging from 0 to 100 mM. The voltage-clamping solutions were supplemented with appropriate concentrations of choline, to provide a cation concentration of 100 mM. All voltage-clamping solutions were of pH 7.4. (*A*) Typical results from a single oocyte showing Na^+ dependence of Q170C steady-state currents, for negative V_t values. The data from the Na^+ titration were transformed to examine Na^+ dependence of the steady-state currents for V_t values, ranging from -150 mV to -10 mV, inclusive. Each curve was fitted with the Hill equation, $I = I_{max} \times [Na^+]^n/([Na^+]^n + K_{0.5}^n)$, where I_{max} = current at -150 mV, to yield values for affinity, K_{Na}, and Hill coefficient, n. (*B*) Voltage dependence of the Na^+ affinity of Q170C. The V_t values from -150 mV to -10 mV, inclusive, are plotted versus [Na^+] on a semilogarithmic scale. Least-squares linear analysis yielded $y = 0.01672x + 3.9298$, SD = 0.45. The inverse of the slope indicates that the K_{Na} varies e-fold per 59.8 mV.

previously (Parent et al., 1992a). The K_{Na} values were then plotted versus the test potentials, with the K_{Na} values presented with the natural logarithm scale (Fig. 3 *B*). Least-squares linear analysis yielded a slope of 0.01672; the inverse of the slope revealed that the fitted K_{Na} values vary exponentially with voltage at a rate of e-fold/59.8 mV.

Since pz locks the transporter at the outside face of the membrane, thereby inhibiting charge transfer (Q), measurement of fractional Q_{max} as a function of phloridzin concentration provides a method of determining pz affinity (K_D). The

Q170C K_D for pz is 1.93 ± 0.08 μM ($n = 4$), which is similar to that of wt rSGLT1, 1.38 ± 0.18 μM ($n = 3$) (data not shown).

In summary, the glutamine-to-cysteine mutation at the 170 site appears to exert little influence over the steady-state behavior of rSGLT1. The affinities of Q170C for Na^+, sugar, and pz are unaltered, and the stoichiometry of the substrates over one transport cycle appears to be unaffected.

Presteady-state behavior of Q170C

Q170C charge transfer characteristics. Fig. 4 compares the mean Q versus V_t curves and calculated Boltzmann relations, of wt ($n = 5$) and Q170C rSGLT1 ($n = 11$). Inspection of Fig. 4 shows that the $V_{0.5}$ for Q170C is shifted to more negative potentials compared to wt (Table 1). The wt $V_{0.5}$ is −1.5 ± 5.1 mV ($n = 5$), whereas the $V_{0.5}$ of Q170C is −13.8 ± 5.5 mV ($n = 11$). This shift in the Q170C $V_{0.5}$ value is statistically significant ($p = 0.001$) and, therefore, indicates an altered voltage sensitivity of the mutated cotransporter, but the shift is not marked. Moreover, there is no significant difference between the dV values of the two species of rSGLT1. The dV values are proportional to the voltage sensitivity of the Boltzmann relations, and are used to derive the apparent valencies, z. Consequently, the apparent valencies of Q170C and wt rSGLT1 are the same (Table 1).

The relative contributions of hyperpolarizing (Q_{hyp}) and depolarizing (Q_{dep}) charges to the overall charge transfer, Q_{max}, reflect the distribution of Q170C, between inward- and outward-facing conformational states at the holding potential

TABLE 1 Comparison of the presteady-state parameters for Q170C and wt rSGLT1

Parameter	wt rSGLT1 ($n = 5$)	Q170C ($n = 11$)	Q170A ($n = 3$)	Q170E ($n = 4$)
Q_{dep}/Q_{max} (%)	86 ± 2	78 ± 4	80 ± 3	92 ± 1
$V_{0.5}$ (mV)	−1.5 ± 5.1	−13.8 ± 5.5	−12.8 ± 4.2	25.1 ± 2.6
dV (mV)	25.7 ± 2.5	27.6 ± 2.7	25.0 ± 4.3	30.3 ± 1.2
z	1.01 ± 0.11	1.08 ± 0.1	0.98 ± 0.14	1.18 ± 0.05

The transient currents of wt and Q170C, Q170A, and Q170E rSGLT1 were integrated to yield the total charge transferred, via the cotransporter, for each V_t. The charge (Q) versus potential (V_t) curves for each rSGLT1 species were fitted with the two-state Boltzmann relation (Eq. 2), enabling the derivation of the presteady-state parameters.

studied. As displayed in Table 1, Q_{dep} comprises ~78 ± 4% ($n = 11$) of the total charge transferred for Q170C. However, for wt rSGLT1, Q_{dep} comprises 86 ± 2% ($n = 5$). This difference is significant at the $p = 0.01$ level. The disparity in the relative charge contribution of Q_{dep}, between Q170C and wt rSGLT1, indicates that occupancy of the outward-facing Na^+ bound conformation of Q170C is less than that of wt rSGLT1, at −50 mV. In other words, the glutamine-to-cysteine mutation at position 170 seems to be affecting the inward/outward-facing distribution of cotransporters.

To investigate this effect more fully, we determined the Na^+ dependence of the relative contributions of Q_{hyp} and Q_{dep} to Q_{max}. Fig. 5 presents the results of a typical single oocyte experiment in which the Na^+ dependence of the Q versus V_t curves of Q170C rSGLT1 was examined over a broad range of [Na^+] values. Since reducing external Na^+ causes proportionate increases in the number of inward-

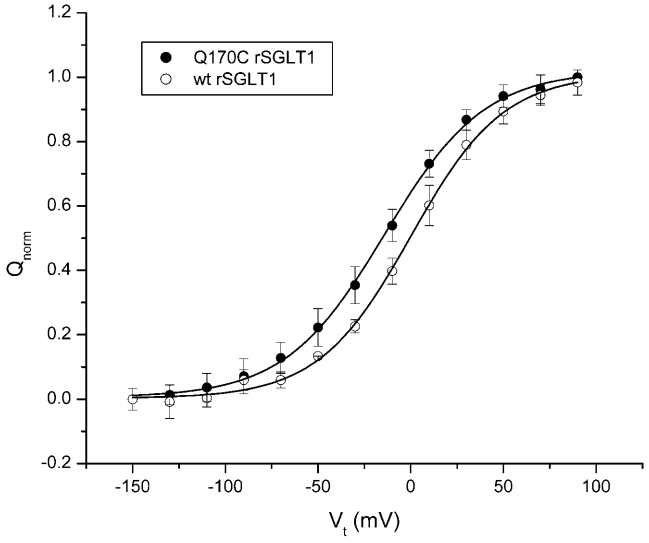

FIGURE 4 Comparison of the mean charge (Q) versus potential (V_t) curves, and the calculated two-state Boltzmann relations, of Q170C and wt rSGLT1. The $Q(V_t)$ curves of Q170C and wt were normalized and zeroed, then the mean charge and SD were calculated for each V_t. The mean charge and SD values were plotted versus V_t. Each curve was then fitted with a two-state Boltzmann relation. All curves were acquired with 100 mM Na^+. The Q170C mean $Q(V_t)$ curve represents 11 oocytes; the wt mean $Q(V_t)$ curve represents five oocytes.

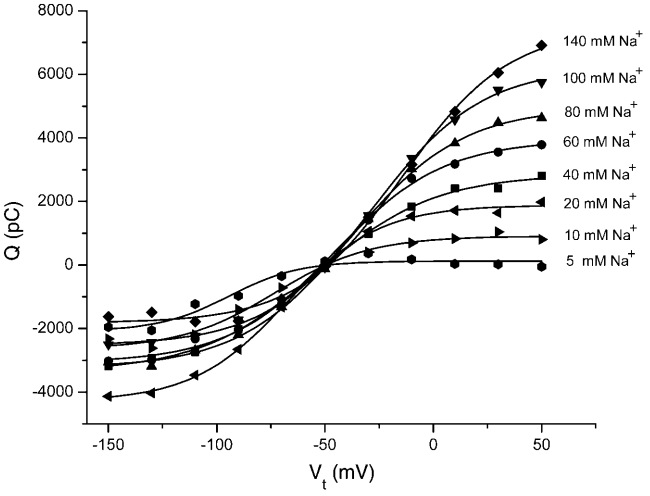

FIGURE 5 The Na^+ dependence of the $Q(V_t)$ curves of Q170C rSGLT1. The results of a representative experiment investigating the effects of [Na^+] upon the $Q(V_t)$ curves of Q170C. The $Q(V_t)$ curves were acquired in the same oocyte for various [Na^+] values. The Na^+ concentrations used were 140 mM, 100 mM, 80 mM, 60 mM, 40 mM, 20 mM, 10 mM, and 5 mM. When possible, the $Q(V_t)$ curves were fitted with a two-state Boltzmann relation.

facing cotransporters, at the −50 mV holding potential, as expected, the fitted Boltzmann relations demonstrate a proportionate decrease in Q_{dep} with decreasing [Na^+]. For conservation of charge we would expect an increase in charge transferred over the hyperpolarizing region. But, as revealed in Fig. 5, Q_{hyp} of Q170C does not show this anticipated increase. In contrast, using an identical protocol for wt rSGLT1, we have found that as Na^+ concentration was decreased, the reduction in Q_{dep} was almost completely offset by an increase in Q_{hyp} (Fig. 6 *B*), and the same is true for the A166C rSGLT1 mutation (Lo and Silverman, 1998b).

The incomplete charge transfer of Q170C compared to wt rSGLT1, with decreasing external [Na^+], suggested that the mutation might be affecting a fundamental functional characteristic of the cotransporter. Therefore, to further explore the observed incomplete charge recovery for Q170C, compared to wt rSGLT1 at hyperpolarizing potentials and low [Na^+], we employed a ramp instead of a step-clamp potential protocol (see Materials and Methods). The ramp protocol slows the presteady-state current response, avoiding saturation of the recording apparatus at early times. Fig. 6 provides a direct comparison of the $Q(V_t)$ curves and Boltzmann relations of Q170C and wt rSGLT1, at [Na^+] values of 10 mM and 100 mM—carried out with the ramp protocol. Similar to the results shown in Fig. 5, Fig. 6 *A* illustrates that a 10 mM Na^+ perfusion solution reduces Q170C Q_{dep} without a corresponding increase in charge in the Q_{hyp} region, resulting in a substantial decrease in the total charge transferred. However, from inspection of Fig. 6 *B*, it is evident that for wt rSGLT1, decreasing Na^+ to 10 mM reduces Q_{dep}, but there is a corresponding increase in Q_{hyp}, resulting in approximate preservation of total charge transferred and a negative shift in the *y* axis. For wt, after normalization, the $Q(V_t)$ for 10 mM Na^+ is 81% of the 100 mM Na^+ curve, over the range from −150 mV to 90 mV. However, for Q170C, the 10 mM Na^+ $Q(V_t)$ represents only 22% of the charge transferred at 100 mM Na^+.

The inability to recover complete charge in the hyperpolarizing region of the $Q(V_t)$ curves with reduced [Na^+] prevents the derivation of an accurate Boltzmann relation. Consequently, it is not possible to confidently calculate $V_{0.5}$ values at low [Na^+], and examination of Na^+ dependence of the $V_{0.5}$ values is precluded.

It is important to note that the marked reduction in charge transfer of Q170C, which occurs with decreasing [Na^+], is not due to loss of transporters from the oocyte membrane. Instead, this apparent loss of charge transfer reflects the tendency of the Q170C mutant to maintain an inward-facing conformation and it would require very large hyperpolarizing potentials (too high to be experimentally feasible) to observe the remaining Q_{hyp}.

Time constants of presteady-state currents for Q170C. Fig. 7 presents a representative decay current of Q170C rSGLT1. Specifically, the decay current is that of a pre-step potential of −30 mV to a post-step potential of 50 mV, with a

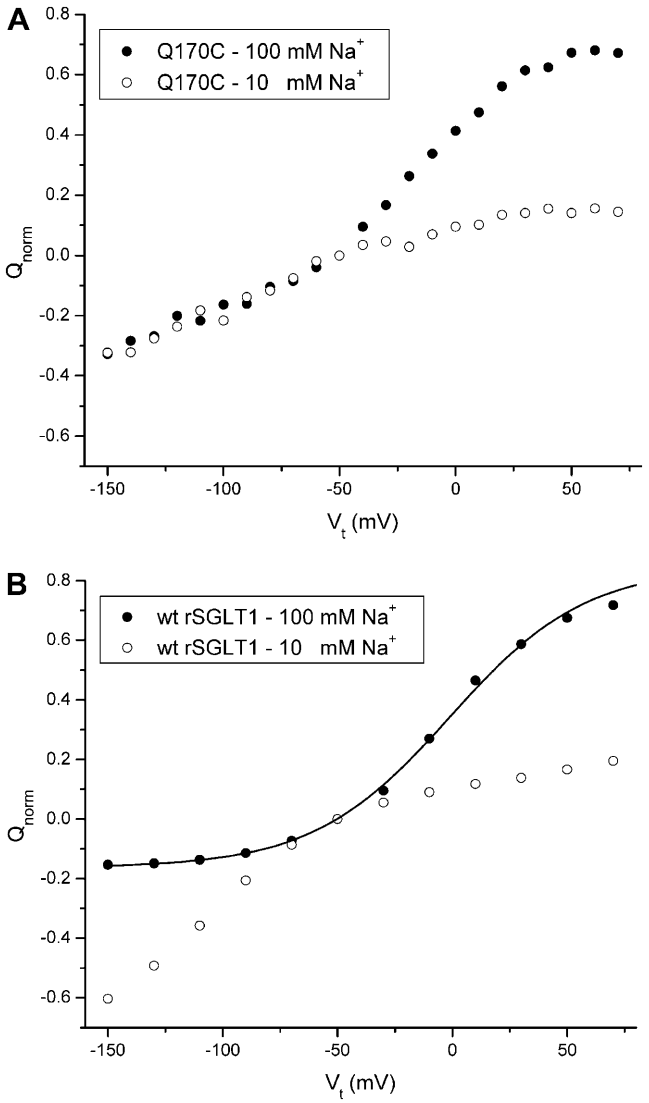

FIGURE 6 Comparison of the effects of 10 and 100 mM Na^+ upon the $Q(V_t)$ curves of Q170C and wt rSGLT1. $Q(V_t)$ curves were acquired for Q170C (*A*) and wt rSGLT1 (*B*), in 10 and 100 mM Na^+. The $Q(V_t)$ curves for both rSGLT1 species were acquired in the same oocyte using a ramp protocol as described in Materials and Methods. When possible, the $Q(V_t)$ curves were fitted with a two-state Boltzmann relation. For wt $Q(V_t)$, at a [Na^+] of 10 mM, there is no saturation at hyperpolarizing potentials over the experimental range tested; therefore, it is not possible to fit the data with a two-state Boltzmann relation.

100 mM Na^+ perfusion solution. As illustrated in Fig. 7, a single time constant is inadequate to describe the presteady-state currents of Q170C; this is evident from inspection of Fig. 7 *A*, which presents the entire current trace. Fig. 7 *B* presents the same current trace, over the range 202–210 ms, and shows to some extent the differences between the second- and third-order fits, although the benefits afforded by the third-order fit are seen much more clearly with the residuals. The residuals of the first-, second-, and third-order exponential fits, derived from Fig. 7, are illustrated in Fig. 8.

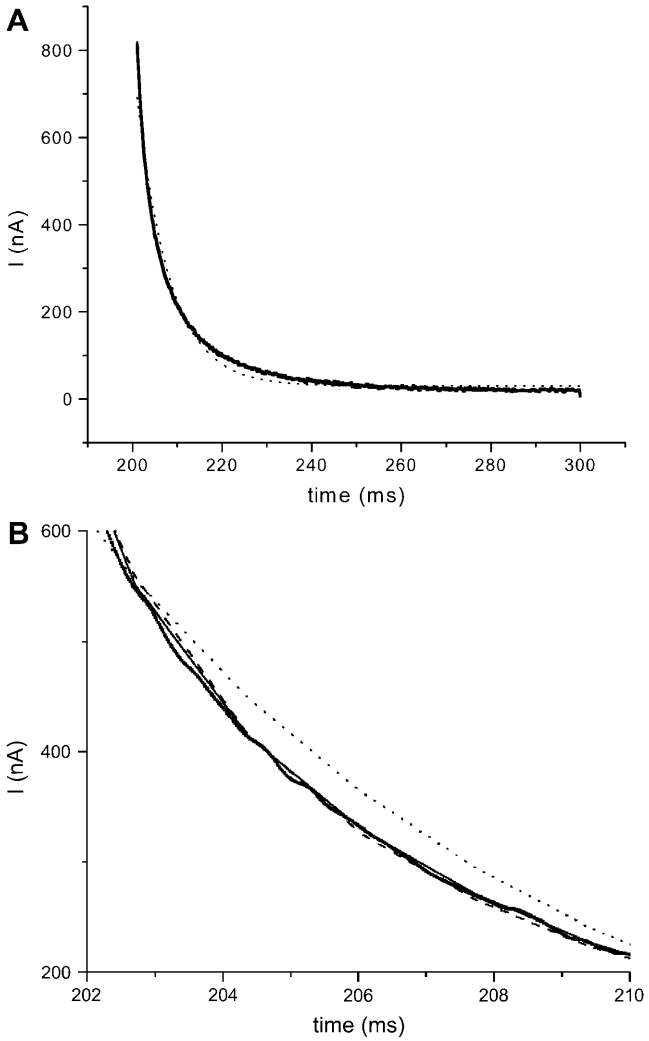

FIGURE 7 A comparison of various orders of exponential decay fits to a transient decay. The transient decay is that of a pre-step potential of −30 mV to a post-step potential of 50 mV. (*A*) First- (*dotted line*), second- (*dashed line*), and third-order (*solid line*) fits are presented with the decay trace. The first-order decay exponential fit is clearly inadequate to describe the transient. (*B*) The decay transient and the exponential fits are presented on a different scale to give a better view of the second- and third-order fits.

The fit residuals are calculated as the difference between measured data and the best fit. Inspection of Fig. 8, *A* and *B*, shows that the residuals of the first- and second-order exponential decay fits have regions that are nonrandom (Fig. 8, *A* and *B*). However, the third-order fit (Fig. 8 *C*) yields a residual comprised entirely of random noise.

Q170C transient currents consistently display third-order decays for all depolarizing V_t traces. The derived decay constants are distinct in their durations, and are denoted accordingly: τ_s, the slow decay constant; τ_m, the medium decay constant; and τ_f, the fast decay constant. The voltage dependencies of the decay constants of Q170C are presented in Fig. 9, with the corresponding decay constants of wt

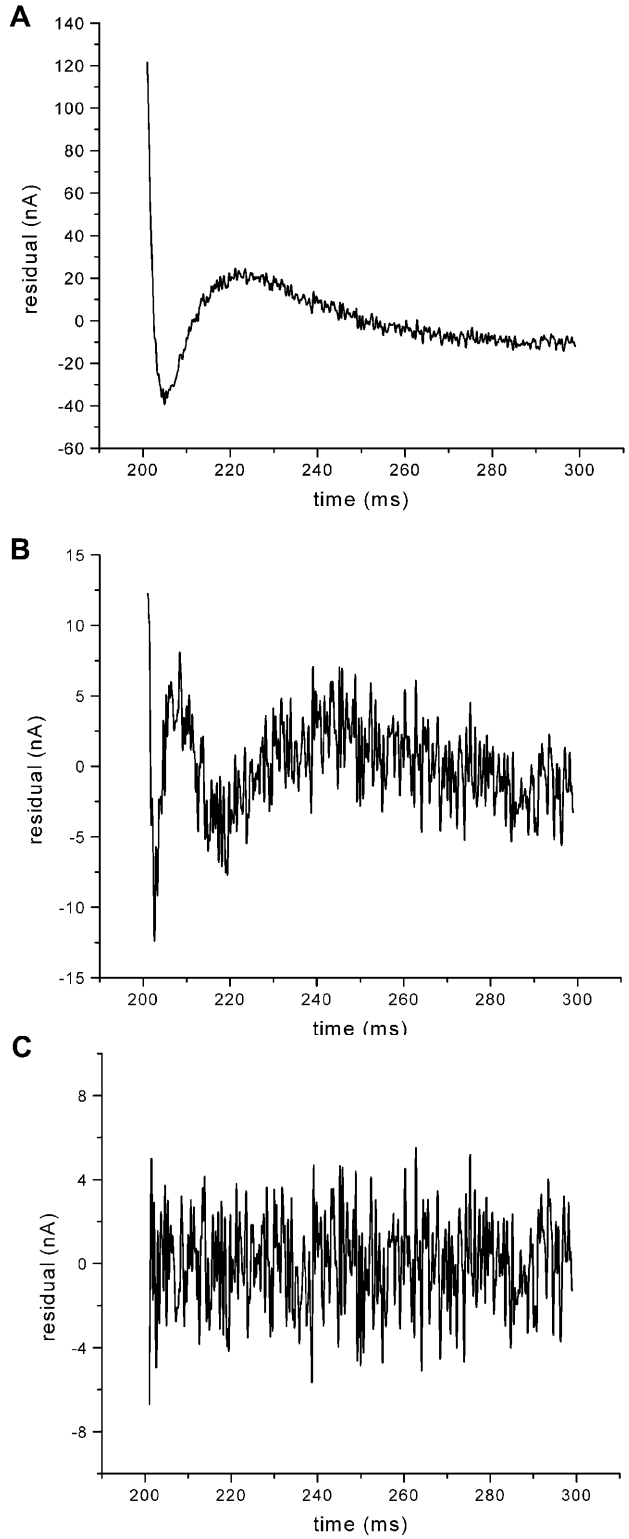

FIGURE 8 The fit residuals. First- (*A*), second- (*B*), and third- (*C*) order fit residuals for the −30 mV pre-step, 50 mV post-step potential transient presented in Fig. 7. The residuals are calculated as *data* − *fit*. A good fit results in noise only, so that the residual oscillates randomly around the zero axis. The residuals of the first- and second-order exponential decay fits have regions, which are nonrandom. However, the third-order fit yields residuals comprised of random noise.

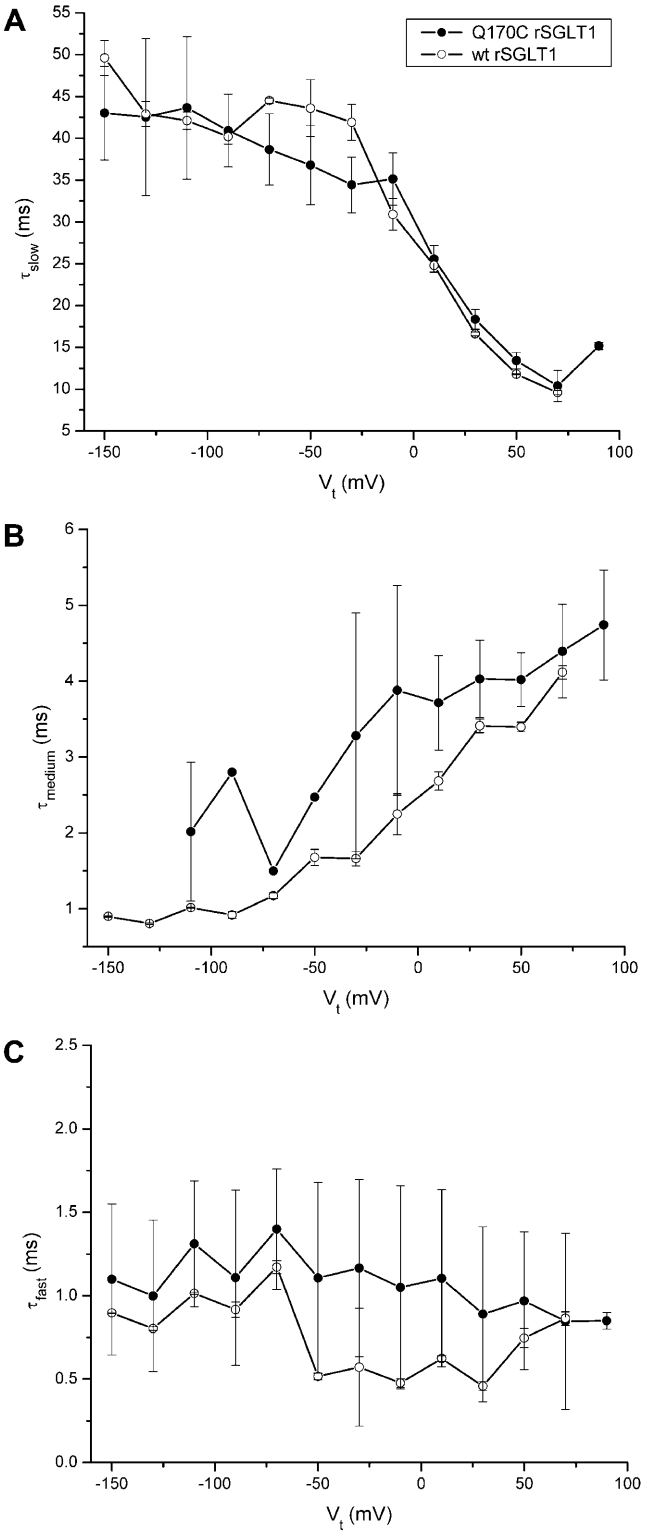

FIGURE 9 A comparison of the decay constants and voltage dependencies of Q170C and wt rSGLT1 transient currents. (*A*) τ_s, Slow decay constant. (*B*) τ_m, Medium decay constant. (*C*) τ_f, Fast decay constant. For wt rSGLT1, $n = 3$, except for -150 mV, -110 mV, -90 mV, and 50 mV, in which $n = 2$. For Q170C rSGLT1, $n = 3$. Error bars represent standard error for data points of $n = 3$, and the mean of the difference for $n = 2$.

rSGLT1. To a reasonable first approximation, there is no difference in the voltage dependence of the three time constants over the range tested. Indeed, the voltage dependence of the three time constants, as a function of external [Na^+], is also very similar for Q170C and wt SGLT1 (data not shown).

It is important to address the validity of the Q170C fast decay. As exhibited in Fig. 9 *C*, the derived Q170C τ_f is voltage-independent and varies from ~0.8–1.4 ms (comparable to the wt rSGLT1 τ_f). This range approximates that of the voltage-clamp. As described in Materials and Methods, the settling time of the voltage-clamp was determined by measuring the oocyte membrane potential as a function of time. Voltage steps ranging from 70 mV to 240 mV were investigated. Final potentials were achieved from 0.6 (70 mV jump) to 1.3 ms (240 mV jump) after the onset of the clamp. Transient currents before the settling of the clamp were removed before fitting, which leaves ~40% of the fast decay component. Three decays are cited as the minimum required to adequately fit a decay exponential. The fastest decay value derived is ~0.8 ms. The amplitude of the fast transition is ~2000 nÅ or greater and the minimum resolution of the system is 5 nÅ, therefore at least six decays are present before the loss of the transient. Consequently, the resolution of the fast component is deemed valid.

Q170C transporter turnover. An estimate of the maximal rate of transporter turnover, k, is calculated using the measured steady-state I_{max} and the presteady-state value Q_{max},

$$k = I_{max} z_{app} / (z_{ss} Q_{max}), \quad (3a)$$

$$= I_{max} / (z_{ss} Ne), \quad (3b)$$

(Loo et al., 1993; Panayotova-Heiermann et al., 1994). The parameters I_{max} and Q_{max} are calculated using an expressing oocyte: I_{max} is the measurement of the maximal steady-state current generated at saturating concentrations of αMG and Na^+, for a V_t of -150 mV; z_{ss} is the steady-state valence, which equals 2, and corresponds to the 2 Na^+ translocated with each transport cycle; and Q_{max} is the value derived by fitting a $Q(V_t)$ curve with a two-state Boltzmann relation. The presteady-state Q_{max} serves as an estimate of expressed cotransporters since $Q_{max} = Nz_{app}e$, with N being the number of cotransporters, z_{app} the apparent valence of the presteady-state model (e.g., the model in Fig. 1 *B*), and e the elementary charge.

In our earlier preliminary survey of Q170C (Lo and Silverman, 1998a), we did not measure turnover relative to wt SGLT1. From our present study, we now show that for Q170C, a turnover value of 11.2 ± 1.7 s^{-1} is derived ($n = 7$). This value should be compared to the wt value of 22.8 ± 0.5 s^{-1} (Lo and Silverman, 1998b). Therefore, the glutamine-to-cysteine mutation significantly reduces cotransporter turnover by ~50%.

The effects of methanethiosulfonate compounds on Q170C functional behavior

We next examined the consequences of reacting Q170C with cysteine-specific sulfhydryl reagents, MTSEA, MTSES, and MTSET. Rabbit SGLT1 has 15 endogenous cysteine residues; none of the native cysteine residues was removed. Recall that neither MTSEA nor MTSES affects the function of wt rSGLT1 (Lo and Silverman, 1998a,b; Vayro et al., 1998).

Effect of MTSES on Q170C steady-state currents

MTSES greatly suppresses sugar-induced inward Na^+ currents. Because of the marked degree of inhibition by MTSES, it was not possible to obtain accurate measurements of sugar-induced Na^+ currents at sugar concentrations below saturation (i.e., <10 mM αMG). However, using sufficiently high expressing oocytes, it was possible to carry out pz titrations before and after exposure to 1 mM MTSES in the same oocyte and obtain estimates of pz K_D. The pz K_D before exposure to MTSES was determined to be 2.8 $\pm$ 1.7 μM, and the K_D after exposure was determined to be 3.4 $\pm$ 2.3 μM ($n = 3$), indicating that MTSES has no effect on phloridzin affinity.

As previously indicated, MTSES inhibits sugar-induced inward Na^+ currents to such a degree that oocytes with exceptional expression of Q170C are required to obtain reliable experimental data at low Na^+ concentrations. We were fortunate to identify such a high expressor and carry out a complete post-MTSES Na^+ titration. We employed a protocol in which the Na^+ titration was carried out before and after MTSES exposure in the presence of 10 mM αMG, in the same oocyte. As shown in Fig. 10 *A*, treatment with MTSES significantly suppresses I_{max} for each of the hyperpolarizing pulses, -150 mV to -50 mV. The value I_{max} was reduced to 36 +/− 3% of the pre-exposure values ($n = 6$). Fig. 10 *B* displays data from the same oocyte used for Fig. 10 *A*, and demonstrates that Na^+ affinity is far less affected by MTSES exposure than is I_{max}. The K_{Na} values before and after MTSES exhibit voltage dependency, and are comparable for V_t values from -90 mV to -10 mV. However, at extreme hyperpolarizing pulses, from -150 mV to -110 mV, MTSES exposure reduces Q170C's affinity for Na^+ by one-half or greater. Exposure to 1 mM MTSES does not alter the apparent stoichiometry of rSGLT1, since the Hill coefficients match those derived in the absence of MTSES.

We also carried out experiments to determine the effect on the Q170C Na^+ leak after MTSES exposure. The Na^+ current at -150 mV is decreased to 45 $\pm$ 2% ($n = 3$) of pre-exposure values (data not shown).

Effect of MTSES on Q170C presteady-state currents

As shown in Fig. 11 *A*, exposure to MTSES results in substantial reduction of the Q170C Q versus V_t curves,

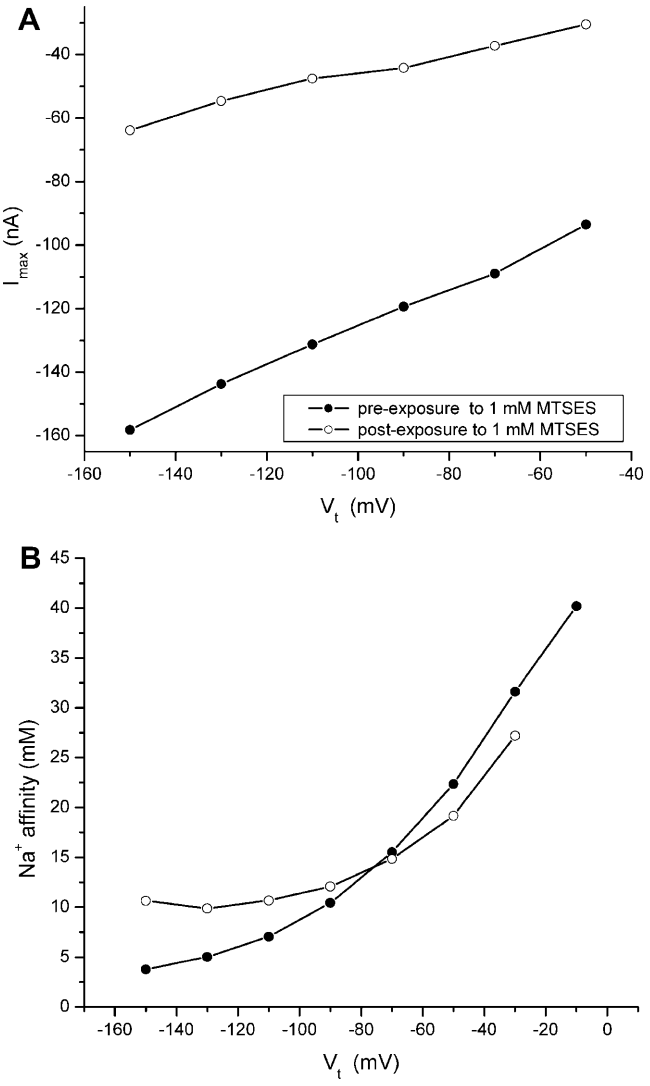

FIGURE 10 The effects of 1 mM MTSES upon the steady-state parameters of a Na^+ titration experiment. Na^+ titrations, as described in the legend of Fig. 3, were performed with the same oocyte, before and after exposure to 1 mM MTSES for 5 min. (*A*) The I_{max} values derived with the Hill equation versus V_t are presented for pre-exposure and post-exposure to MTSES. (*B*) K_{Na} vs. V_t are presented for pre-exposure and post-exposure to MTSES.

which is reversed by treatment with 10 mM dithiothreitol (DTT). Although MTSEA has no effect upon Q170C function, prior exposure to MTSEA prevents the action of MTSES, and the MTSEA protection is reversed by DTT (data not shown). To exclude the possibility that MTSEA reacts with hydrophobically located native cysteines to bring about a conformational change, which alters MTSES accessibility to the 170 position, we performed protection experiments using the membrane-impermeant, cationic MTSET. As shown in Fig. 11 *B*, exposure to MTSET completely prevents MTSES reaction with Q170C, but MTSET has no effect on Q170C maximum charge transfer.

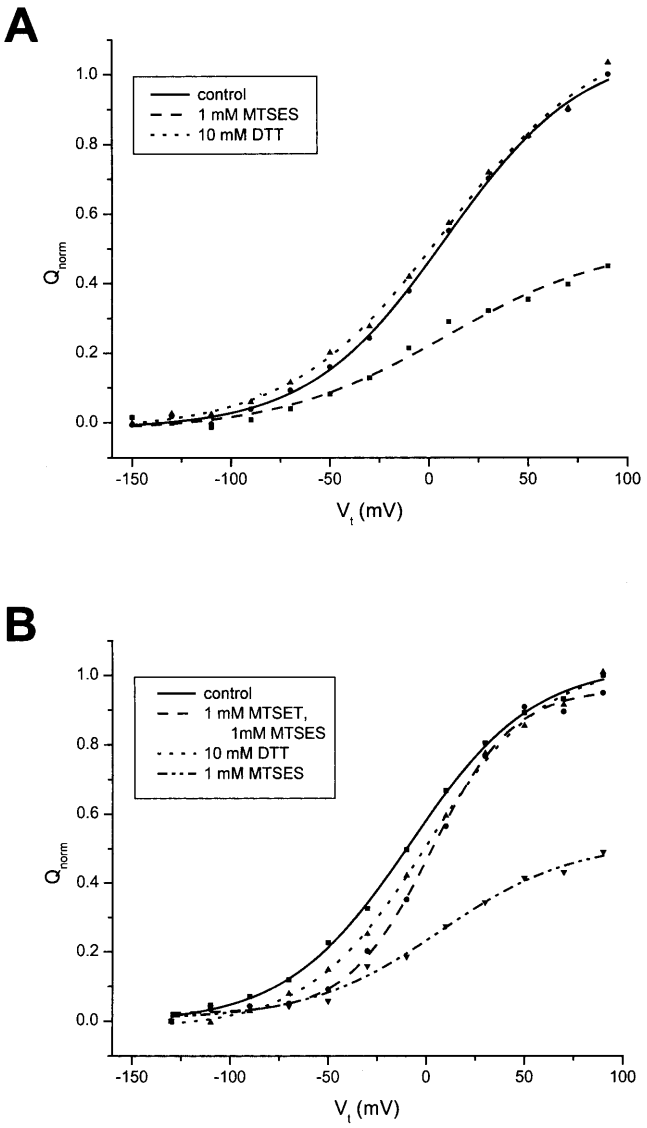

FIGURE 11 Effects of MTSES, MTSEA, and MTSET on charge transfer of Q170C. Typical results demonstrating the effects of sulfhydryl-specific reagents on Q170C charge transfer. The protocols, for each panel, were carried out in the same oocyte. (*A*) After documenting the Q vs. V_t behavior under control conditions (——), the oocyte was superfused with 1 mM MTSES (·····) for 5 min, followed by 10 mM DTT for 10 min (·····). Data have been normalized to the control. (*B*) Q vs. V behavior under control conditions was determined (——), followed by MTSET for 5 min, washed with voltage-clamping solution, superfused with 1 mM MTSES for 5 min, washed, and Q vs. V determined (·····). Next, the oocyte was superfused with 10 mM DTT for 10 min, washed, and Q vs. V measured (·····). Finally, the oocyte was superfused with 1 mM MTSES for 5 min, washed, and Q vs. V obtained (·····). All curves were normalized to control.

MTSET protection is reversed after exposure to 10 mM DTT. Given that MTSET reactivity is restricted to externally accessible native cysteines in SGLT1, we conclude that MTSET protects against MTSES accessibility to the cysteine mutation introduced at the 170 position (which is located in the putative external loop joining TMs IV–V), by directly reacting (modifying) the cysteine at that site. We conclude that both cationic MTSEA and MTSET react with Q170C and that the inhibitory effect of MTSES on charge transfer is a consequence of the anionic ethylsulfonate group added at the 170 position. The fact that DTT completely reverses the inhibitory effect of MTSES within minutes suggests that reduction in charge transfer by MTSES is not due to a change in the number of surface-expressed Q170C transporters. To confirm this, using methods previously established for wt SGLT1 and an A166C rSGLT1 mutant (Vayro et al., 1998), we verified that the number of [^{3}H]phloridzin binding sites in COS-7 cells transfected with Q170C, before and after treatment with MTSES, was the same (data not shown).

Several other protection experiments were performed with Q170C expressed in *Xenopus* oocytes and it was verified that the inhibitory effect of MTSES on Q170C function was independent of Na^+ or prior exposure to 200 μM phloridzin.

The effects of MTSES upon the various presteady-state parameters of Q170C are displayed in Table 2. Exposure to 1 mM MTSES reduces total charge transfer by ~50% over the voltage range, −150 mV to +90 mV. Further, similar to what occurs when [Na^+] is reduced (see Figs. 5 and 6), there is a preferential inhibitory effect upon the charge transfer at depolarizing voltages. In a paired comparison of five different oocytes, before and after MTSES exposure, the Q_{dep} contribution to total charge transferred was found to be 82 ± 2% in the five oocytes tested, and this contribution is reduced to 73 ± 3% after MTSES exposure (Table 2). This difference is significant at the $p = 0.01$ level, but only accounts for ~10% of the observed ~50% reduction in Q_{max}. The majority of the ''loss'' in charge transfer in the presence of MTSES occurs because of a failure to recover charge transfer in the hyperpolarizing region over the range of observation, up to −150 mV. This behavior is similar to what is observed when [Na^+] is reduced (Figs. 5 and 6), in the absence of MTSES, and is a direct consequence of the fact that under both reduced external Na^+, and after reaction with MTSES, the transporter occupancy of its inward-facing conformation states is substantially increased. More complete charge recovery would require extending the hyperpolarization beyond −150 mV, a range not feasible experimentally. Because of the incomplete charge recovery over the hyperpolarization region, it is not possible to

TABLE 2 Effects of 1 mM MTSES on the presteady-state parameters of Q170C rSGLT1

Parameter	pre-MTSES	post-MTSES
Q_{total} (%)	100	44 ± 13
Q_{dep}/Q_{total} (%)	82 ± 2	73 ± 3

The charge (Q) versus potential (V_t) curves of Q170C rSGLT1, were acquired before and after exposure to 1 mM MTSES for 5 min in the same oocyte. Q_{total} refers to the total charge transferred within the experimental range, −150 mV to 90 mV. The pre-MTSES Q_{total} values correspond to Q_{max}.

determine the Boltzmann for Q170C post-MTSES and, consequently, estimation of the effect on $V_{0.5}$ and dV is precluded.

After Q170C exposure to MTSES, the substantial reduction in transient currents made it difficult to resolve the three decay constants, τ (slow, medium, fast), for potentials more hyperpolarizing than -10 mV. Nevertheless, there appeared to be no significant difference in the τ-values, comparing pre- and post-MTSES conditions from -10 to 70 mV (data not shown).

Effect of MTSES on carrier turnover

Turnover was calculated before and after a 5-min exposure to 1 mM MTSES, in the same oocytes ($n = 4$). The pre-MTSES turnover was 12.7 ± 1.32 s^{-1}; the post-MTSES turnover was found to be 4.9 ± 1.89 s^{-1}. This ~60% post-MTSES reduction, observed in the present study, contradicts our earlier published result (Lo and Silverman, 1998a), in which we reported that MTSES exposure did not appear to change Q170C turnover. However, the present investigation, performed with oocytes of significantly higher Q170C expression, clearly demonstrates that Q170C turnover is, indeed, substantially reduced. In fact, after reaction with MTSES, the Q170C turnover is approximately less than one-fourth that of wt rSGLT1 (wt turnover $= 22.8 \pm 0.5$ s^{-1}). Of interest, the reduction in turnover, due to MTSES, can be reversed by exposure to DTT. In two different oocytes, pre-MTSES exposure turnover averaged 11.8 s^{-1}; after MTSES, turnover was reduced to 3.4 s^{-1}; and after 10 min exposure to 10 mM DTT, the turnover was measured at 13.4 s^{-1}. These estimates of turnover are calculated using direct measurements of I_{max} at -150 mV and Q_{total}, before and after exposure to MTSES. In the equation for turnover, the total Q serves as an estimate of the number of cotransporters, N, expressed at the oocyte surface (Eq. 3a). However, as noted in previous sections, the measured total Q, post-MTSES, is an underestimate because of incomplete charge recovery. We note that exposure to 1 mM MTSES causes a 70% reduction in I_{max}. Since N, the number of transporters, is in fact unchanged, and z, the net charge transported per cycle (i.e., 2), is likewise the same, the turnover is, in fact, proportional to I_{max} (Eq. 3b).

We sought to corroborate this measurement using the COS-7 cell system transiently transfected with Q170C. The maximal velocity (V_{max}) of [^{14}C]αMG uptake at 10 mM αMG concentration, pre- and post-MTSES exposure, was determined and the ratio was calculated to be ~2.6. Since the number of Q170C transporters at the surface, as measured by phloridzin binding in COS-7 cells, was the same pre- and post-MTSES, the ratio of V_{max} pre- and post-MTSES should be a reliable measure of turnover number under the same conditions. The COS-7 cell measurements suggest that the turnover of Q170C has been reduced, post-MTSES exposure, by ~80%. The COS-7 cell measurements, therefore, represent independent confirmation that the post-MTSES turnover is proportional to I_{max}, i.e., at least ~60–70% reduced. In summary, the glutamine-to-cysteine mutation at the 170 position reduces the cotransporter turnover by ~50%, and treatment with MTSES further reduces the Q170C turnover time by another 60–70%, so that Q170C post-MTSES is more than fourfold slower than wt SGLT1.

The effects of glutamine-to-alanine and glutamine-to-glutamate mutations at 170

To corroborate the observed effects of Q170C and Q170C post-MTSES on SGLT1 function, the presteady-state parameters of Q170A and Q170E rSGLT1 were examined. Q170A was examined to probe neutrality, for comparison with Q170C; Q170E was employed to investigate the effects of negative charge, for comparison with MTSES-reacted Q170C. The mean $Q(V_t)$ curves for Q170A and Q170E were normalized and fitted with the Boltzmann relation. The data for Q170A and Q170E are presented with those of wt and Q170C (Fig. 12, Table 1).

The mean $Q(V_t)$ curve and the fitted Boltzmann relation of Q170A closely mirror those of Q170C (Fig. 12). As presented in Table 1, the various presteady-state parameters of Q170C and Q170A are equivalent. The Q_{dep}/Q_{max} values of Q170C and Q170A are $78 \pm 4\%$ ($n = 11$) and $80 \pm 3\%$ ($n = 3$), respectively. As with Q170C, the Q170A Q_{dep}/Q_{max}

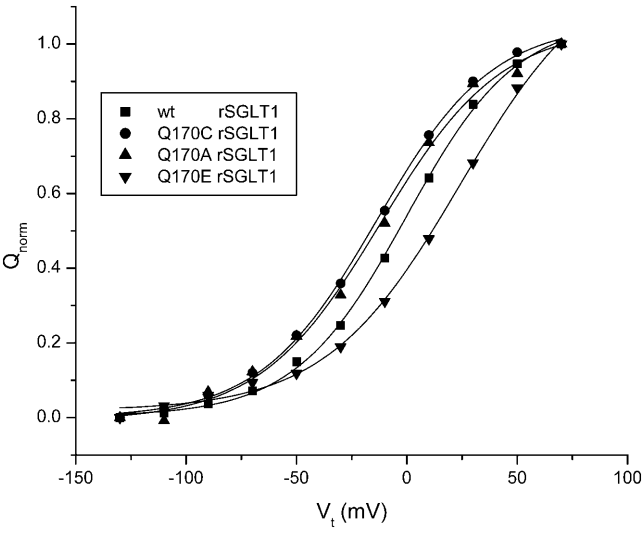

FIGURE 12 Comparison of the mean charge (Q) versus potential (V_t) curves, and the calculated two-state Boltzmann relations, of Q170C, Q170A, Q170E, and wt rSGLT1. The $Q(V_t)$ curves of Q170C, Q170A, Q170E, and wt were normalized and zeroed, then the mean charge and SD were calculated for each V_t. The mean charge and SD values were plotted versus V_t. Each curve was then fitted with a two-state Boltzmann relation. All curves were acquired with 100 mM Na^+. The Q170C mean $Q(V_t)$ curve represents 11 oocytes; the Q170A mean $Q(V_t)$ curve represents three oocytes; the Q170E mean $Q(V_t)$ curve represents four oocytes; and the wt mean $Q(V_t)$ curve represents five oocytes.

value is significantly different from the wt value ($p < 0.01$). The Q_{dep}/Q_{max} values of Q170C and Q170A indicate comparable cotransporter conformational distributions at $V_h = -50$ mV, with a greater proportion of transporters at the inside-facing conformation, compared to wt. The $V_{0.5}$ value for the Q170C Boltzmann is -13.8 ± 5.5 mV ($n = 11$), versus the $V_{0.5}$ value for Q170A of -12.8 ± 4.2 mV ($n = 3$), verifying an equivalent voltage sensitivity. Finally, the z-values of the two mutants are comparable: Q170C $z = 1.08 \pm 0.11$, versus Q170A $z = 0.98 \pm 0.14$ (Table 1). Neutrality at 170, therefore, appears to exert significant influence on empty carrier kinetics.

The $Q(V_t)$ curve of Q170E demonstrates saturation in the hyperpolarizing region (Fig. 12), therefore a Boltzmann relation can be fitted to the data and the appropriate parameters can be derived (Table 1). Although a direct comparison cannot be drawn to Q170C post-MTSES, Q170E offers insight into the effects of a negative charge at 170. As displayed in Table 1, the Q170E Q_{dep}/Q_{max} is $92 \pm 1\%$, which is significantly different from the wt value of $86 \pm 2\%$ ($p = 0.0005$). The Q170E mutation, therefore, elicits a cotransporter conformational distribution with a greater number of cotransporters at the *outside*-facing conformation, compared to wt, at $V_h = -50$ mV. This greater Q170E Q_{dep} contribution, compared to wt, is opposite to the trend of the neutral mutants Q170C and Q170A. The Q170E $Q(V_t)$ curve and fitted Boltzmann relation show a shift of $V_{0.5}$ to positive potentials with a mean value of 25.1 ± 2.6 mV ($n = 4$). The negative charge of the glutamate does not have a significant effect upon the z (Table 1). Q_{hyp} saturation and an unchanged z-value suggest that the Q170E mutation has very little effect upon the charge transfer, unlike MTSES-reacted Q170C. Whereas, Q170A exhibits a $Q(V_t)$ curve shifted to a negative potential, the presence of a negative glutamate shifts the $Q(V_t)$ curve to a significantly positive potential. This positive shift suggests an increased Na^+ affinity.

The carrier turnover values were calculated for the Q170A and Q170E rSLGT1 mutants. The turnover value for Q170A was calculated to be 9.6 s^{-1} ($n = 1$) and the turnover for Q170E is 11.6 ± 2.5 s^{-1} ($n = 4$). This is comparable to the reduction in turnover observed for Q170C (11.2 ± 1.7 s^{-1} ($n = 7$)). Interestingly, the reduction in turnover, elicited by the Q170E mutation, is not as great as the reduction in turnover observed for MTSES-reacted Q170C. Therefore, although replacement of polarity at 170 with neutrality or negative charge serves to significantly reduce turnover, the structure of the side chain bearing the negative charge appears to modify the extent of turnover reduction.

DISCUSSION

The rationale for exploring the functional characteristics of Q170C in greater depth was to explain its anomalous behavior relative to the cysteine mutants of adjacent residues 163, 166, and 173, which together, form part of the Na^+ binding and voltage-sensing domain of rSGLT1 (Lo and Silverman, 1998a,b).

Charge specificity of chemical modification by MTS sulfhydryl reagents is one characteristic that distinguishes Q170C from the other loop mutants. For A166C (Lo and Silverman, 1998a,b) and for F163C and L173C (M. Silverman, unpublished data), the anionic MTS derivative, MTSES, reacts with the cysteine at the mutated position, but does not affect transport—whereas the cationic MTSEA markedly alters transport activity (Lo and Silverman, 1998a,b). The opposite is true for Q170C; both MTSEA and MTSET react with the cysteine at the 170 position and block MTSES, yet neither has functional consequence. This charge specificity perhaps indicates that the loop region has a complexity beyond the primary structure, with an intricate tertiary structure.

These studies, as well as previous studies by Lo and Silverman (1998a,b) demonstrated that the MTS compounds do not alter wt rSGLT1 function. It is, therefore, reasonable to assume that the effects of these MTS reagents are due to reaction with the exogenous cysteines introduced in the various mutants. In the present investigation, there remains a legitimate question concerning the mechanism of MTSET and MTSEA protection against Q170C exposure to MTSES. Two scenarios for protection are possible. The first mechanism of observed MTSET and MTSEA protection against MTSES exposure involves binding of the MTSEA and MTSET with the cysteine at the 170 position, thereby directly blocking MTSES reaction. A possible second mechanism could involve the limiting of MTSES accessibility to the 170 position, through an indirect conformational change occurring in response to MTSET or MTSEA reacting with one or more of the native cysteines, putatively located in an extracellular position (i.e., C255, C345, C351, C355, and C361). Although such indirect effects might be attributable to MTSEA protection, MTSET is membrane-impermeant and therefore would be expected to interact with both native extracellular cysteines as well as with the extracellular cysteine introduced at the 170 position. We conclude that it is the presence of a negative ethylsulfonate group at the 170 position, arising out of reaction with MTSES, that causes altered function of the chemically modified Q170C.

Even more intriguing are the marked qualitative differences in function that occur in Q170C after exposure to MTS reagents compared to A166C, F163C, and L173C. We have previously shown that exposure to MTSEA shifts the $V_{0.5}$ of each of the single cysteine mutants F163C, A166C, and L173C to negative potentials (Lo and Silverman, 1998a,b). Further, progressively greater negative shifts in potential are observed for the combination of double- and triple-cysteine mutants created at these three positions (Lo and Silverman, 1998a). Moreover, Q_{max} under these conditions remains constant (Lo and Silverman, 1998a). This behavior (i.e., shift of $V_{0.5}$ to more negative potentials with no change in Q_{max})

mimics the effect of progressively lowering the external Na^+ concentration (Lo and Silverman, 1998a). Collectively, these results lead us to conclude that 163, 166, and 173 together form part of the Na^+ binding and voltage-sensing domain of rSGLT1.

In contrast to the observed $V_{0.5}$ shift to negative potentials described above with no change in Q_{max}, exposure of Q170C to MTSES produces almost the opposite results—i.e., a substantial decrease in measured charge transfer over the voltage range from −150 to +90 mV, which precludes an accurate derivation of Boltzmann parameters, such as $V_{0.5}$.

The results of this study provide new insights into the conformational states and transitions that underlie rSGLT1 function. This conclusion is based on several behavioral characteristics of Q170C compared to wt rSGLT1:

1. In general, the relative magnitudes of charge transferred at hyperpolarizing pulses, Q_{hyp}, and depolarizing pulses, Q_{dep}, to the total charge transferred, Q_{max}, reflect cotransporter conformational state distribution at the holding potential, V_h. Our data show that for Q170C, depolarizing pulses contribute less charge to Q_{max} than do depolarizing pulses to wt rSGLT1 Q_{max}. This reduced Q_{dep} indicates that at steady state, fewer Q170C transporters are in the outside-facing, Na^+ bound state, and more are redistributed among the other conformational states. Thus replacement of the polar glutamine, with a relatively nonpolar and bulky cysteine, serves to drive the Q170C equilibrium, at $V_h = -50$ mV, toward the inside-facing conformation.
2. Lower [Na^+] should favor a distribution of cotransporters toward inside-facing conformation, resulting in a reduced Q_{dep}. As expected, our experiments (Figs. 5 and 6 *A*) show that reduced Na^+ concentrations proportionately decrease the Q_{dep} region of Q170C. However, if carrier reorientation to the outside is unaffected by the mutation, we would expect that any loss of Q_{dep} would be regained in the Q_{hyp} region. This would manifest as a negative shift in the Boltzmann relation along the *y* axis leading to a substantial increase in charge transfer at hyperpolarizing voltages. This is precisely what is observed for wt at 10 mM Na^+ (Fig. 6 *B*). The fact that this is not observed in the case of Q170C (Fig. 6 *A*), where reduced [Na^+] results in a preferential reduction in Q_{dep}, implies that empty carrier reorientation to the outside-facing conformation is significantly retarded for Q170C, compared to wt SGLT1.
3. Exposure to 1 mM MTSES reduces the $Q(V_t)$ curves of Q170C, via a preferential effect upon the Q_{dep}. But after reaction with MTSES, there is no increase in charge transfer at hyperpolarizing potentials. It is noteworthy that the effect of MTSES on Q170C mimics that of decreasing [Na^+]—i.e., both appear to reduce the total charge transferred. However, since K_{Na} of Q170C is unchanged, the implication is that addition of an anionic ethylsulfonate at the 170 position affects a potential dependent transition of empty (non-Na^+-bound) carrier. This once again argues for a steady-state cotransporter distribution, which favors maintenance of the inward-facing conformation and further suggests that anionic charge at the 170 position enhances this localization.
4. The most profound effect of a change of polarity and charge at the 170 position in rSGLT1 is the reduction in transporter turnover number. The enhanced expression levels, which we were able to achieve in the present study, by coinjection of the Q170C cDNA together with plasmid-bearing mouse T-antigen, have allowed us to carry out more quantitative evaluation than we were able to accomplish in our earlier investigations of Q170C function (Lo and Silverman, 1998a). Our new findings convincingly demonstrate that replacement of glutamine with cysteine at 170 causes a reduction in turnover by a factor of 2 compared to wt rSGLT1. Also, reaction of Q170C with MTSES produces a further decrease of >50% in turnover. Therefore, MTSES-reacted Q170C exhibits a turnover, which is more than four times slower than wt rSGLT1.

Many of the observed effects of altered polarity and charge at the 170 residue, elicited with the Q170C mutation and subsequent reaction with MTSES, were confirmed with Q170A (neutral) and Q170E (anionic) mutations.

The glutamine-to-alanine mutation generated $Q(V_t)$ curves that correspond closely to those of Q170C. Q170A and Q170C have comparable $V_{0.5}$ values, Q_{dep}/Q_{max} values, and turnover numbers, which are reduced in both mutations by ~50%, compared to wt.

The glutamine-to-glutamate mutation, Q170E, had interesting consequences on presteady-state behavior. There was a substantial positive shift in the $V_{0.5}$ of the Boltzmann relation, with little change in *z* compared to wt. Taken together with the shift in $V_{0.5}$ to negative voltages observed for Q170A and Q170C, without a significant change in *z* (Table 1), the implication is that change in polarity and charge at position 170 affects the Na^+-binding and voltage-sensing properties of the transporter. This behavior is similar but opposite to that described for the F163C, A166C, and L173C single, double, and triple mutants reacted with cationic MTSEA (Lo and Silverman, 1998a,b). A positive charge on residues at the 163, 166, and 173 positions inhibits Na^+ binding (negative charge has no effect), a negative charge at position 170 increases Na^+ binding, but a positive charge (i.e., reaction with MTSEA or MTSET) has no effect. The statistically significant increase in Q_{dep}/Q_{max} observed for Q170E, implies a greater distribution of cotransporters in an outside-facing conformation, compared to wt at $V_h = -50$ mV, also consistent with increased binding affinity for Na^+. Collectively, these data suggest that the glutamine at position 170 lies in the Na^+ permeation pathway. Another observation, which implicates a Na^+ permeation pathway localization of 170, is the fact that anionic MTSES reduces the Q170C Na^+ leak.

Lo and Silverman previously demonstrated that replacement of an alanine with a cysteine at 166 effects a ~50% reduction in turnover number (Lo and Silverman, 1998b). Although the cysteine mutation at 166 mimics the effects of cysteine mutation at 170, the mutation does not duplicate the shift in residue polarity; i.e., alanine to cysteine is a neutral to neutral mutation, unlike glutamine to cysteine, which is polar to neutral. Further, a charge-dependent effect on A166C turnover number was observed, which is opposite to that found for 170. Specifically, a positive point charge at 170 has no effect, but a negative point charge significantly reduces substrate turnover. For the 166 cysteine mutant, a positive ethylamine group causes a significant reduction in turnover. Therefore, although mutations at both the 166 and 170 positions influence empty carrier kinetics and participate in Na^+ interaction, a border exists there that delineates charge specificity.

Just as a precise spatial organization appears to exist in the loop region, from 163 to 173, with two regions delineated with a border of charge specificity, there also appears to be an emerging spatial organization to the more immediate environment surrounding Q170. This Q170 spatial organization is made evident by the differential effects of Q170C, Q170A, Q170E, and Q170C after exposure to MTSES. Replacement of polarity with neutrality, via the Q170C and Q170A mutations, caused a substantial and equivalent change in voltage sensitivity and a reduction in turnover number. Neither MTSEA- nor MTSET-reacted Q170 had an effect upon cotransporter function; therefore a positive charge is benign. However, a negative charge, as observed with Q170C post-MTSES and Q170E, generated a profound reduction in turnover number. Although the turnover trend was similar, what was particularly informative was the differential effect that Q170C post-MTSES and Q170E had upon function. The negative charge of Q170E caused a reduction in turnover, equivalent to Q170C and Q170A. After MTSES exposure, Q170C caused a reduction in turnover that was approximately twofold greater than Q170C, Q170A, and Q170E. This difference in turnover reduction could be due to two different mechanisms. The first involves the degree to which the negative charge can extend out from the cotransporter backbone. In this case, the negative charge of the ethylsulfonate group likely has a greater radius of mobility than the negative charge of the glutamic acid. Perhaps the ethylsulfonate is able to move closer to a critical area in the three-dimensional Q170 region. Another possible mechanism involves a modifying effect by the polar disulfide bond of the MTS-reacted Q170C upon the negative charge of the ethylsulfonate. Either scenario indicates a charge-specific spatial sensitivity in the immediate Q170 environment.

The Q170E mutant yielded valuable insights. For Q170E, z is not significantly different from that of wt or Q170C. Since the apparent valence represents the formal charge moved through the electric field of the membrane, the fact that an added negative charge at 170 is without significant consequence upon z, suggests that the 170 position moves very little during cotransporter charge transfer. Perhaps this indicates that the residue at 170 influences charge transfer and turnover by serving as a *hinge* or a *gate* that moves very little during function. The finding that MTSET reacts with the cysteine at Q170C but has no effect demonstrates that steric hindrance is insufficient to explain the effects. Unfortunately, a direct comparison cannot be drawn between the $V_{0.5}$ values of Q170C post-MTSES and Q170E, because of our inability to fit a Boltzmann relation to MTSES-reacted Q170C. Nevertheless, what is clear is that rather than an effect on Na^+ binding, reaction of Q170C with MTSES has a profound effect on charge transfer. Thus the Q170C post-MTSES effects also point to position 170 being located in the vicinity of a segment with the properties of a voltage sensor.

The Q_{dep}/Q_{max} values of the investigated Q170 mutants offer insight into empty carrier kinetics. The two neutral mutants, Q170C and Q170A, exhibit a significant decrease in Q_{dep} contribution compared to wt rSGLT1. The negative mutant Q170E, however, shows a significant increase in Q_{dep} compared to wt. This suggests that cotransporter distribution is influenced by polarity and charge at 170. Neutrality drives cotransporter distribution toward inside facing. Moreover, the Na^+ dependence of the Q170C Q_{dep} contribution to total charge transferred, Q_{total}, implies that once at the inside-facing conformation, cotransporters do not easily move back to outside-facing conformation. Q170E results indicate that negative charge causes a cotransporter redistribution to outside facing. Thus polarity and charge affect the carrier distribution and reorientation, which is reflected in the reduced turnover values of Q170C, Q170C post-MTSES, Q170A, and Q170E.

A final consideration, concerning the reduced turnover number, involves the aspect of the rate-limiting step. Collectively, our findings imply that modification of charge and polarity at the 170 position in rSGLT1 has a profound effect on certain rate-limiting step(s) in cotransporter function. In an attempt to localize the transition state(s) that are being affected by the mutation at the 170 position, we sought to compare the presteady-state behavior of wt rSGLT1 with that of Q170C and with Q170C reacted with MTSES. The transient currents of Q170C rSGLT1 clearly possess multiorder exponential decay, a characteristic also demonstrated by the transient currents of wt hSGLT1 (Chen et al., 1996) and wt rSGLT1 (Krofchick and Silverman, 2003). Q170C transient currents are well resolved with third-order exponential decay, for V_t values from -30 mV to 90 mV. Third-order exponential decay, applied within this experimental range, consistently generates three decay constants that closely correspond to those of wt rSGLT1 (Krofchick and Silverman, 2003). Both Q170C and wt rSGLT1 have a slow decay (voltage-dependent, $\tau_s = \sim$10–40 ms), a medium decay (voltage-dependent, $\tau_m = \sim$1.5–6 ms), and a fast decay (voltage-independent, $\tau_f = \sim$0.5–1.5 ms).

Chen and co-workers, in 1996, reported two decay components for hSGLT1, even with zero *trans* Na^+, and

attributed both decay components to empty carrier transitions. The Na^+ and voltage dependencies of Q170C rSGLT1 τ_s and τ_f are very similar to those reported by Chen's group for wt hSGLT1 (Chen et al., 1996), and Krofchick and Silverman (2003) for wt rSGLT1. The voltage dependence of the slow decay of Q170C exhibits a sigmoidal shape, very similar to the sigmoidal shapes of the voltage dependencies of the slow decays of wt hSGLT1 (Chen et al., 1996) and wt rSGLT1 (Krofchick and Silverman, 2003). The magnitude of the fast decay component of Q170C, as well as its voltage-independence, is also very similar to the fast decay components of wt hSGLT1 (Chen et al., 1996) and wt rSGLT1 (Krofchick and Silverman, 2003). The Na^+ and voltage-dependent data of Q170C rSGLT1 and wt rSGLT1 τ_s and τ_f, therefore, suggest that these transitions correspond to the empty carrier transitions of wt hSGLT1, determined by Chen et al. (1996).

A plausible candidate for the rate-limiting step of SGLT1 is the slow transition (Fig. 1 *B*) $C_2 \Leftrightarrow C_3$. Although the Q170C mutation reduces turnover number by ~50% compared to wt, there is no change in any of the decay constants, including τ_s. Similarly, analysis of the time constants after reaction of Q170C with MTSES also shows no significant change compared to pre-MTSES or wt values. We conclude that altered polarity and charge at the 170 glutamine position of rSGLT1 affect a cotransporter conformational transition; this is rate-limiting but probably not associated with reorientation of empty carrier (i.e., the affected transition is not accounted for by any of the transitions depicted in Fig. 1 *B*). This conclusion is consistent with the proposal of Parent and coworkers, who suggested that the rate-limiting step of hSGLT1 is the Na^+ binding/debinding event of the inside-facing conformations (Parent et al., 1992b). This latter transition is excluded from the four-state system depicted in Fig. 1 *B*, and would not contribute to the decay components of the transient currents. If the inside-facing Na^+ binding/debinding transition is indeed the rate-limiting step, this might explain why the Q170C mutation and the exposure of Q170C to MTSES causes a reduction in turnover and a tendency toward occupancy of inside-facing conformation.

On the basis of this study, we conclude that the glutamine at 170 is of profound importance to rSGLT1 function. Further investigations into the Q170 residue and the region adjacent, should provide greater insight into the behavior of the Na^+/glucose cotransporter.

The authors acknowledge R. Reithmeier, D. Clarke, P. Backx, R. Tsushima, and V. Khutorsky for helpful discussion.

This work was supported by a grant to M. Silverman (FRN-15267) as part of the Canadian Institutes of Health Research Group in Membrane Biology (FRN-25026).

REFERENCES

Chen, X. K., M. J. Coady, and J. Y. Lapointe. 1996. Fast voltage clamp discloses a new component of presteady-state currents from the Na^+-glucose cotransporter. *Biophys. J.* 71:2544–2552.

Costa, A. C. S., J. W. Patrick, and J. A. Dani. 1994. Improved technique for studying ion channels expressed in *Xenopus* oocytes, including fast superfusion. *Biophys. J.* 67:395–401.

Hediger, M. A., M. J. Coady, T. S. Ikeda, and E. M. Wright. 1987. Expression cloning and cDNA sequencing of the Na^+/glucose cotransporter. *Nature.* 330:379–381.

Krofchick, D., and M. Silverman. 2003. Investigating the conformational states of the rabbit Na^+/glucose cotransporter. *Biophys. J.* 84:3690–3702.

Lo, B., and M. Silverman. 1998a. Cysteine scanning mutagenesis of the segment between putative transmembrane helices IV and V of the high affinity Na^+/glucose cotransporter SGLT1. *J. Biol. Chem.* 273:29341–29351.

Lo, B., and M. Silverman. 1998b. Replacement of Ala-166 with cysteine in the high affinity rabbit sodium/glucose transporter alters transport kinetics and allows methanethiosulfonate ethylamine to inhibit transporter function. *J. Biol. Chem.* 273:903–909.

Loo, D. D., A. Hazama, S. Supplisson, E. Turk, and E. M. Wright. 1993. Relaxation kinetics of the Na^+/glucose cotransporter. *Proc. Natl. Acad. Sci. USA.* 90:5767–5771.

Panayotova-Heiermann, M., S. Eskandari, E. Turk, G. A. Zampighi, and E. M. Wright. 1997. Five transmembrane helices form the sugar pathway through the Na^+/glucose cotransporter. *J. Biol. Chem.* 272:20324–20327.

Panayotova-Heiermann, M., D. D. Loo, C. T. Kong, J. E. Lever, and E. M. Wright. 1996. Sugar binding to Na^+/glucose cotransporters is determined by the carboxyl-terminal half of the protein. *J. Biol. Chem.* 271:10029–10034.

Panayotova-Heiermann, M., D. D. Loo, M. P. Lostao, and E. M. Wright. 1994. Sodium/D-glucose cotransporter charge movements involve polar residues. *J. Biol. Chem.* 269:21016–21020.

Parent, L., S. Supplisson, D. D. Loo, and E. M. Wright. 1992a. Electrogenic properties of the cloned Na^+/glucose cotransporter. I. Voltage-clamp studies. *J. Membr. Biol.* 125:49–62.

Parent, L., S. Supplisson, D. D. F. Loo, and E. M. Wright. 1992b. Electrogenic properties of the cloned Na^+/glucose cotransporter. II. A transport model under nonrapid equilibrium conditions. *J. Membr. Biol.* 125:63–79.

Taglialatela, M., L. Toro, and E. Stefani. 1992. Novel voltage clamp to record small, fast currents from ion channels expressed in *Xenopus* oocytes. *Biophys. J.* 61:78–82.

Vayro, S., B. Lo, and M. Silverman. 1998. Functional studies of the rabbit intestinal Na^+/glucose carrier (SGLT1) expressed in COS-7 cells: evaluation of the mutant A166C indicates this region is important for Na^+-activation of the carrier. *Biochem. J.* 332:119–125.

Zampighi, G. A., M. Kreman, K. J. Boorer, D. D. Loo, F. Bezanilla, G. Chandy, J. E. Hall, and E. M. Wright. 1995. A method for determining the unitary functional capacity of cloned channels and transporters expressed in *Xenopus laevis* oocytes. *J. Membr. Biol.* 148:65–78.